aerospace

MDPI

Article

Large-Scale Path-Dependent Optimization of Supersonic Aircraft

John P. Jasa [1,*], Benjamin J. Brelje [1], Justin S. Gray [2], Charles A. Mader [1] and Joaquim R. R. A. Martins [1]

[1] Aerospace Engineering, University of Michigan, Ann Arbor, MI 48109, USA; bbrelje@umich.edu (B.J.B.); cmader@umich.edu (C.A.M.); jrram@umich.edu (J.R.R.A.M.)

[2] PSA Branch, NASA John H. Glenn Research Center, Cleveland, OH 44135, USA; justin.s.gray@nasa.gov

* Correspondence: johnjasa@umich.edu

Received: 23 September 2020; Accepted: 15 October 2020; Published: 20 October 2020

Abstract: Aircraft are multidisciplinary systems that are challenging to design due to interactions between the subsystems. The relevant disciplines, such as aerodynamic, thermal, and propulsion systems, must be considered simultaneously using a path-dependent formulation to assess aircraft performance accurately. In this paper, we construct a coupled aero-thermal-propulsive-mission multidisciplinary model to optimize supersonic aircraft considering their path-dependent performance. This large-scale optimization problem captures non-intuitive design trades that single disciplinary models and path-independent methods cannot resolve. We present optimal flight profiles for a supersonic aircraft with and without thermal constraints. We find that the optimal flight trajectory depends on thermal system performance, showing the need to optimize considering the path-dependent multidisciplinary interactions.

Keywords: multidisciplinary design optimization; trajectory optimization; aircraft design; thermal systems design

1. Introduction

Aerospace systems are *path-dependent*, and this feature must be considered to accurately assess system performance. We use the term path-dependent here to refer to any system where the time history of system state affects performance. Critical path dependencies include short-term effects, such as aircraft component temperatures, and long-term effects, such as the structural fatigue accumulated in the airframe from previous missions. For instance, if engineers ignored the aircraft's time-dependent thermal history when designing the thermal management subsystems, they would inaccurately estimate the aircraft's capabilities. Making steady-state assumptions at individual operating points ignores thermal transients that might be performance-limiting, leading to non-optimal design. Optimizing the design and trajectory of an aircraft considering path-dependent effects results in better overall performance than optimizing the trajectory of a fixed-design aircraft due to the coupling between aircraft design and mission performance. For instance, modeling both the design and trajectory simultaneously accurately resolves the interdisciplinary trade-offs between the thermal constraints and heat generation, which leads to better aircraft performance.

The earliest published study on path-dependent optimization of aircraft was performed by Kaiser [1] in 1944, though solving path-dependent optimization problems became much more widespread through the use of computers. Kaiser hand-solved the minimum time-to-climb problem using an analytic expression for the energy-state tradeoffs for piston-powered aircraft [1]. Specifically, he plotted velocity-altitude contours and found the optimum climb profile graphically, where optimal climb speeds can be found by drawing straight-line segments orthogonally to the contour lines [1].

In the 1950s and 60s, researchers computed optimal trajectories for many air and space applications, especially high-speed military vehicles, including rockets, supersonic aircraft, and planetary vehicles [2–5]. Some of these papers solved for the optimal trajectories using gradient-based algorithms [4,5], which were some of the first works to incorporate numerical optimization into the study of path-dependent problems. In all of these papers, the vehicle designs were fixed and only the trajectories were being optimized.

A seminal paper by Bryson and Denham [6] detailed the steepest ascent method for solving optimum programming problems using the adjoint method. In the 1970s and 1980s, path-dependent optimization evolved through the inclusion of path constraints, uncertainty quantification, and advanced controller theory, as detailed by Bryson in a review article [7]. Most of this work focused on gradient-based coupled structural and control optimization to improve vehicle dynamic response to disturbances [8–11]. Although these studies were limited in the number of disciplines they considered, they serve as the basis for multidisciplinary optimization of coupled system in a path-dependent manner.

Contemporary work has both expanded the number of disciplines considered and increased the fidelity of the physical analysis methods. Multiple publications from the Air Force Research Laboratory (AFRL) detail their path-dependent MDO capabilities, which include propulsion, thermal management, electrical systems, stability, aerodynamics, economics, and overall utility [12–17]. Some terms that these works introduce are *multi-parameter performance*, which enables broader analysis of aircraft performance [14], and *effectiveness-based design*, which determines mission effectiveness objectives through physics-based analysis rather than proxies like aircraft weight or fuel burn, as detailed by Clark Jr et al. [17]. AFRL researchers developed these methodologies to more accurately assess the complete performance of the aircraft by having holistic vehicle-level metrics instead of single-discipline objectives.

Some of the most relevant preceding work to this paper comes from AFRL concerning optimization of the thermal management system (TMS) in a path-dependent context [18–23]. The present work differs because the mission profile is represented by continuous design variables, which allows for entirely flexible flight profiles that are not represented by pre-defined segments. Examining the AFRL work in detail, Alyanak and Allison [19] design a fuel thermal management system (FTMS) and show that thermal transients affect optimal system architecture and aircraft performance. They modeled mission segments using prescribed fuel fractions, used fixed thermal loads in each segment, and sized the FTMS using analytic expressions for temperature states with assumed efficiencies. They show that the studied aircraft's weight increases by 282% when considering the flight heat loads and thermal constraints. Although they admit that the result is unrealistic due to the simplicity of the thermal system architecture, it does show the impact that thermal constraints have on aircraft sizing [19].

Recently, NASA has been performing mission-based MDO as part of its Transformational Tools and Technologies project at its Glenn and Langley Research Centers. Falck et al. [24] and Hendricks et al. [25] implemented a collocation-based approach for solving multidisciplinary trajectory problems that efficiently solves both the time integration and optimization problem simultaneously. Schnulo et al. [26] used that same approach to optimize the X-57 electric aircraft flight demonstrator across a full mission with multiple flight segments. Falck and Gray [27] continued by developing the mission optimization tool, Dymos, and investigating its use and scalability for MDO problems. Hendricks et al. [28] demonstrated the tool's capabilities by optimizing the aerostructural, propulsive, and electric performance of a tiltwing urban air mobility vehicle.

This work presented in this paper is inspired by Falck et al. [24] and Hendricks et al. [25], who coupled mission optimization with propulsion analysis and thermal constraints. Their work showed that by using a higher-order collocation method with gradient-based optimization and analytic derivatives, fully coupled mission problems are tractable. Falck et al. [24] specifically examined how path-dependent thermal constraints affect the optimal mission profile of an electric aircraft,

an application case that necessitates the use of fully coupled mission and design optimization. Although individual disciplinary analyses could be performed to evaluate the aircraft performance, a fully coupled model more accurately resolves the interdisciplinary trade-offs between the thermal constraints and heat generation.

At the same time that AFRL and NASA were expanding their mission optimization capabilities, the MDO Lab at the University of Michigan was approaching similar problems from multiple different angles [29–33]. Liem et al. [29,34,35] sought to maximize aircraft performance by considering multiple representative missions with different payloads and ranges. Kao et al. [30,31] developed a modular adjoint-based approach to optimize the mission profile for a commercial airliner for multiple missions simultaneously. They used surrogate models for aerodynamic and propulsion data to make the mission optimization tractable.

Brelje and Martins [36] developed an aircraft conceptual design tool, OpenConcept. This tool models many subsystems within the aircraft, including the propulsion, electrical, and thermal systems, and can be used to optimize the states of the aircraft across its mission [36,37]. Simultaneously, Chauhan and Martins [38] developed a method to optimize electric vertical takeoff and landing aircraft trajectories and presented multiple optimal trajectories for a tandem tiltwing aircraft. Jasa et al. [39] performed mission optimization of a morphing wing commercial airliner. They then applied that mission optimization method to a supersonic interceptor and added thermal constraints [40]. Most recently, Hwang et al. [33] performed fully coupled allocation-mission-design of a commercial airliner. Their work included Reynolds-averaged Navier–Stokes (RANS) computational fluid dynamics (CFD) in the loop, 128 missions, and a ticket-selling economics model to maximize the profit for a given airline considering a new aircraft design.

This paper moves towards considering more physical disciplines simultaneously with trajectory optimization methods to design aircraft more efficiently. Beyond the work dedicated to solving path-dependent problems, methods developed for large-scale design optimization are used in this paper. Developments from the MDO community provide the foundation for some of these methods, including the ADjoint approach [41–44], different MDO strategies [45,46], and MAUD [47]. By combining approaches from the fields of trajectory optimization and large-scale MDO, we can solve complex path-dependent problems.

In this paper, we construct and assemble a multidisciplinary model that can analyze and optimize the performance of an aircraft across a full mission. We then optimize a large-scale aero-thermal-propulsion-mission problem for a representative supersonic aircraft and show that the optimal flight trajectory is tightly coupled to the thermal system performance. By capturing these multidisciplinary trades within the large-scale optimization problem, we show that both flight trajectory and aircraft design must be considered simultaneously to maximize vehicle performance. This differs from previous path-dependent mission research because the flight profile parameterization allows flexible optimal solutions that cannot be obtained using pre-defined mission segments, which leads to higher aircraft performance.

We study a combination of disciplines using aerodynamic data constructed from CFD evaluations, propulsion performance from one-dimensional cycle analysis tools, and thermal system models. These models are combined within NASA's OpenMDAO framework and we use gradient-based optimization with efficiently computed derivatives to enable these large-scale design studies. The techniques presented in this paper are useful for MDO practitioners who want to efficiently optimize large-scale multidisciplinary systems.

This paper is organized as follows. In Section 2, we discuss the disciplinary models used. We explain the optimization methodology and problem formulation in Section 3. We then present and discuss the optimization results in Section 4.

2. Disciplinary Models

In this section, we describe the individual flight dynamics, aerodynamic, propulsion, and thermal models used in this work. In combination, they comprise the multidisciplinary model we used for optimization.

2.1. Flight Dynamics

To discuss how path-dependent problems can be solved, we need to develop the equations that dictate the time-varying properties of the system. These ordinary differential equations (ODEs) are used to model the behavior of any subsystem across time. For physical objects moving through space, the most common ODEs are the equations of motion. Depending on the application, relevant terms within these ODEs can include effects from gravity, engine thrust, wing lift and drag, and electromagnetic forces. To obtain the thermal states of the aircraft, we need ODEs that track component temperature, coolant flow and temperature, and air flow through heat exchangers. We need an ODE for any time-varying state that we are interested in monitoring throughout the optimization process. In this chapter, we focus on the equations of motion that dictate how aircraft move through space.

The unsteady aircraft equations of motion for 2D planar flight are

$$m\dot{V} = T\cos\alpha - D - W\sin\gamma, \tag{1}$$

$$mV\dot{\gamma} = L + T\sin\alpha - W\cos\gamma, \tag{2}$$

$$\dot{h} = V\sin\gamma, \tag{3}$$

$$\dot{x} = V\cos\gamma, \tag{4}$$

where L, D, T, and W are the forces of lift, drag, thrust, and weight respectively, m is the mass of the aircraft, V is the aircraft velocity, γ is the flight-path angle, h is the altitude, x is the horizontal distance, and α is the angle of attack. Figure 1 shows how these forces are oriented relative to an aircraft in flight.

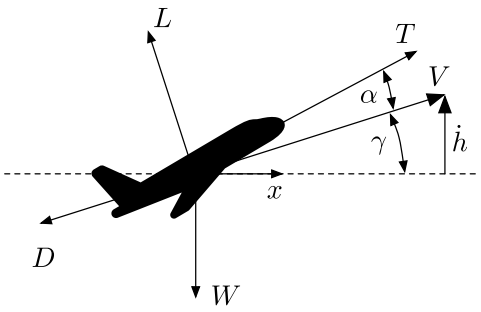

Figure 1. Free-body diagram for the forces acting on an aircraft used in the equations of motions.

2.2. Aerodynamic Modeling

The Efficient Supersonic Air Vehicle (ESAV) aircraft provides a common research model for an advanced military fighter aircraft configuration, and has been studied before using MDO with a variety of disciplines, including aerodynamics, structures, stability, mission, noise, and emissions [48–51]. To obtain the aerodynamic properties of the aircraft, we constructed a mesh for RANS CFD of the aircraft, which we evaluated at a range of different flight condition to generate an aerodynamic surrogate model. In this work, the shape of the aircraft was held fixed, so we do not need to perform physics-based analysis in the loop to update the aerodynamic properties as the aircraft design changes. This greatly reduces the computational cost of running the optimization.

We began with a surface definition of the aircraft as provided by Lockheed Martin. We plugged the engine inlet and nozzle and removed control surface gaps to simplify the model. These simplifications

are possible in this context because we are only considering the aerodynamic properties of the vehicle at different flight conditions without assessing the effects of control surfaces or coupled aeropropulsive effects.

The RANS solver used in this work is ADflow [52], a structured finite-volume CFD code with overset capabilities using an implicit hole cutting scheme [53]. The geometry was meshed using on overset mesh made up of 10 blocks and a total of 2,185,600 cells. We converge the flow solution using the approximate Newton–Krylov solution algorithm [54]. We use the Spalart–Allmaras turbulence model and the fluxes are discretized with central-differencing. Two nominal flow solutions for the aircraft, one at Mach = 0.8 and the other at Mach = 1.5, are shown in Figure 2.

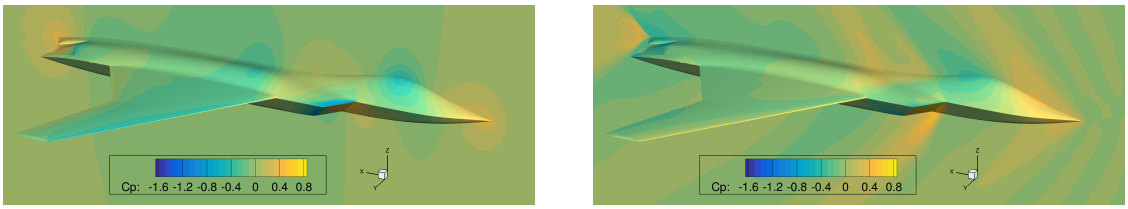

(**a**) (**b**)

Figure 2. Two flow solutions of the ESAV geometry at nominal flight conditions. The colormap shows the C_P, or coefficient of pressure, a dimensionless number describing the relative pressures in the flow field. (**a**) Flow solution at $\alpha = 2$ and Mach = 0.8; (**b**) Flow solution at $\alpha = 2$ and Mach = 1.5.

Although we could use this CFD model directly in the optimization problem and perform an analysis at each point needed in the mission simulation, we can instead construct a surrogate model based on many training points using data from the CFD analyses (run offline). We uniformly query the three-dimensional Mach-α-altitude space to populate the surrogate training points, and obtain C_L and C_D as outputs from the CFD analysis. We use 13 points in the Mach direction, from 0.2 to 1.8, clustered around the transonic region, 7 points from -8 to 8 degrees α, and 3 points in the altitude space between 0 and 20,000 m for a total of 273 CFD evaluations.

We use this data to construct a surrogate model using Surrogate Modeling Toolkit (SMT) (https://github.com/SMTorg/smt) [55], which provides a variety of methods to represent data sets. We chose to use the RMTS method [56] because of its inexpensive training and evaluation costs for low-dimensional input spaces and because it provides gradients of the outputs with respect to the inputs efficiently. Figure 3 shows an angle of attack and Mach sweep of the aerodynamic model at an elevation of 30,000 feet.

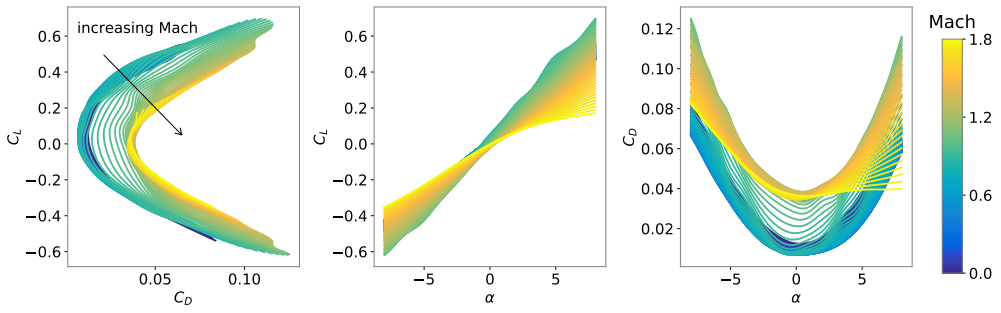

Figure 3. Drag polar and aerodynamic properties for the ESAV aircraft obtained from the CFD-trained surrogate model at an elevation of 30,000 feet with a Mach sweep from 0 to 1.8, and an α sweep from $-8^\circ$to 8°.

2.3. Propulsion Systems

For modeling the propulsion systems in the ESAV aircraft, we constructed a generic supersonic engine model in pyCycle (https://github.com/openmdao/pycycle) [57]. pyCycle is a tool that was

developed by NASA to facilitate the exploration of unique propulsion system designs within a multidisciplinary vehicle context. Specifically, pyCycle solves the 1D thermodynamic equations for conservation of mass, momentum, and energy needed to model an engine. pyCycle models the same physics as the industry standard tool, Numerical Propulsion System Simulation (NPSS), but provides analytic derivatives, is open-source, and has been verified against NPSS in a series of papers [57,58]. pyCycle is written in OpenMDAO, which helps support modular model construction and integration into larger MDO problems. Our engine model was based on an existing NPSS model of the GE F110 engine obtained from NASA. We adapted the NPSS model for use in pyCycle by translating its architecture and element maps. The engine design parameters are shown in Table 1.

Table 1. Design parameters for the supersonic engine model.

Parameter	Value	Units
Design altitude	35,000	ft
Design Mach number	0.8	
Design T_4	3200	$^\circ$ R
Design thrust	15,000	lbf
Extraction ratio	1.05	
Fan pressure ratio	3.3	
HPC pressure ratio	9.7	

We need to give the engine model a good set of initial guesses for its state values because its internal Newton-based solvers are extremely sensitive to the solver starting point. If we simply ran the engine model without feeding it reasonable initial guesses, it would diverge on the first iteration. We could hardcode guesses into the model, but that would not account for the differences in converged states of the engine at different flight conditions, let alone if we change the engine design. To remedy this, we developed a process to generate surrogate-enhanced guess tables that can provide good initial guesses to the engine model that are independent of the model's previous state. The process is outlined below for a given engine design:

1. Run the engine at the fixed design point and an off-design point
2. Save the resulting states and performance data
3. Train the surrogate model using the saved states data
4. Repeat steps 1–3 for all points in the flight envelope by varying the off-design analysis point flight conditions

After going through this process across the range of conditions in the flight envelope, we now have a surrogate model that we can query to give good initial guesses to the engine model. We sweep the flight condition space in three dimensions: Mach, altitude, and combustor exit temperature. Even if we change the static design of the engine, this enhanced guess table gives reasonably good initial guesses, allowing us to also optimize the engine. Figure 4 shows the training points and thrust outputs for the engine model at full throttle. The engine model flight envelope shown in Figure 4 is not limited by the aerodynamic loads. Instead, the flight envelope is constrained by the flight dynamics model in the full optimization problem, which has limits on the speed and altitude allowed during the mission.

In addition to providing good initial guesses for the engine model, the surrogate model also provides performance information for the engine based on the flight condition and throttle. This allows us to query the surrogate model instead of the actual engine model when performing mission analysis and optimization with a fixed engine design. Because the surrogate model and the actual engine model have the same inputs and outputs, we can choose to use either method within a given model with ease. For this work, because we are holding the engine design fixed and are focused on the mission and thermal systems design, we use the surrogate model within the mission optimization. If we were to vary the engine design, we would need to regenerate the propulsion surrogate model or call the

engine model directly, which would increase the computational cost of the optimization. Each call the to the engine analysis takes approximately five seconds on a 2.8 GHz quad-core desktop, which means that generating the full engine surrogate model requires approximately two hours.

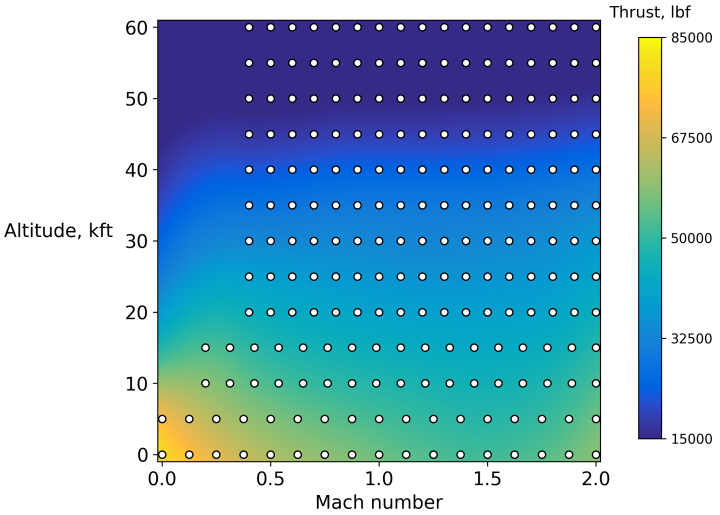

Figure 4. The surrogate training points and thrust outputs for the mixed-flow turbofan engine model.

2.4. Thermal Systems

Using a modular thermal systems framework will allow designers to quickly prototype new architectures without needing to solve for all the ODEs of interest. In general, designers do not know *a priori* what the best architecture will be for a given aircraft application because thermal loads comes from many sources at different temperatures within an aircraft. The order of the coolant tanks, heat exchangers, sources, and sinks directly affects the thermal system, its efficacy, and weight. Also, using a different architecture is a discrete design choice, so it is challenging to examine this using gradient-based optimization. The thermal system designer must use their expertise to select architectures to study.

To model the modular thermal system, we use OpenConcept (https://github.com/mdolab/openconcept/), an aircraft conceptual design and optimization toolkit that is built using OpenMDAO and includes simple, conceptual-level models of systems components [36]. OpenConcept can model conventional and electric propulsion components and recent development has extended OpenConcept's capabilities to include thermal management systems [37]. In this work, we use the heat exchanger, transient reservoir, mixer, splitter, and thermal lifting system groups from OpenConcept. The physics and implementation of these components have been detailed by Brelje et al. [37]. We construct a modular thermal system here based on a simple architecture for the ESAV aircraft, shown in Figure 5. It is a dual-tank FTMS where the fuel is heated by an on-board aircraft component before either being used in the engine burner or recirculated back into the feed tank. During recirculation, the fuel goes through a ducted heat exchanger whose cold side interfaces with ducted airflow. Here, we assume that there is an inlet-duct-nozzle separate from the full engine so we do not need to model the entire engine to examine this thermal system. The dual tank system allows the main fuel tank to not be affected by the thermal dissipation and recirculation as the recirculating fuel only enters the feed tank.

There are many parameters that must be set within the model. The relevant values used in these studies are provided in Table 2. For the heat exchangers, we assume aluminum fins and casings and obtain fin and channel dimensions from a representative aircraft air-liquid heat exchanger. The coolant used throughout this thermal work and in the engine burner is Jet-A fuel [59]. We assume standard atmospheric air enters the inlet and flows through the bypass duct.

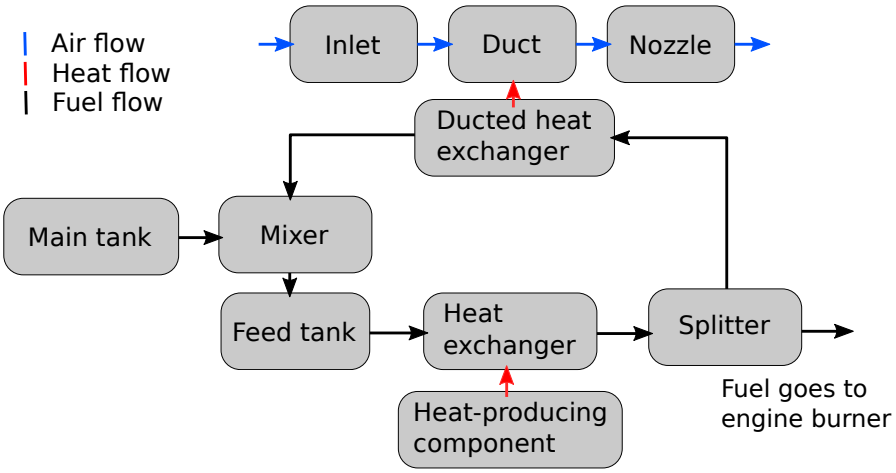

Figure 5. Dual tank modular FTMS used for part of this work.

Table 2. Specifications and parameter values for the dual tank thermal system.

Parameter	Value	Units	Comments
Initial tank temperatures	300	K	
Initial feed tank fuel mass	1000	kg	
$\dot{m}_{\text{transfer}}$	3.	kg/s	
$\dot{m}_{\text{recirculated}}$	1.	kg/s	
Specific heat of component	921	J/kg/K	aluminum
Specific heat of fuel	2010	J/kg/K	Jet-A
Fuel density	800.	kg/m^3	Jet-A
Fuel thermal conductivity	0.110	W/m/K	Jet-A
Fuel viscosity	0.000704	kg/m/s	Jet-A
Component mass	12	kg	small avionics package
Channel width	1.0	mm	
Channel height	20.	mm	
Channel length	0.2	mm	
Case thickness	2.0	mm	
Fin thickness	0.102	mm	
Plate thickness	0.2	mm	
Material thermal conductivity	190	W/m/K	aluminum
Material density	2700	kg/m^3	aluminum
Number of fins long, cold side	3	–	
Number of channels wide, cold side	200	–	
Number of hot/cold stacks	15	–	
Channel height, cold side	14	mm	
Channel width, cold side	1.35	mm	
Fin length, cold side	6	mm	
Specific heat, cold side	1005	J/kg/K	air
Thermal conductivity, cold side	0.02596	W/m/K	air
Viscosity, cold side	0.00001789	kg/m/s	air
Channel height, hot side	1	mm	
Channel width, hot side	1	mm	
Fin length, hot side	6	mm	
Specific heat, hot side	2010	J/kg/K	Jet-A
Thermal conductivity, hot side	0.11	J/kg/K	Jet-A
Duct inlet area	0.0645	m^2	
Nozzle throat area	0.0194	m^2	

In Figure 5, the inlet, duct, and nozzle are modeled using pyCycle and the rest of the thermal elements are modeled using OpenConcept. The elements in this thermal system are able to interface

directly because both pyCycle and OpenConcept are implemented in OpenMDAO. In general, the computational cost of the OpenConcept elements is much smaller than that of the pyCycle elements. The coolant loop only deals with liquid fuel, whereas the duct passageway concerns potentially supersonic air with full chemical equilibrium analysis. We could simplify the inlet, duct, and nozzle elements, but by not doing so we are able to use the pyCycle elements off-the-shelf. This also allows the thermal system to interface directly with the engine model in future work.

This thermal model has a large number of possible inputs and settings that will affect the cooling performance of the FTMS. The tank temperatures, fuel mass, heat-producing component temperatures, thermal limits, fuel flow rates through the loop and feed pipes, must all be considered when evaluating the system effectiveness. Given a real aircraft, we could set up the thermal system to match that configuration and then provide thermal data and inputs for different flight conditions. However, to keep this work available in the public domain, we use nominal values based on thermal loads that a current-gen supersonic jet might see.

Many factors influence the heat transfer through the bypass duct for a fixed flight condition, including inlet and nozzle duct areas, the temperature of the coolant entering the heat exchanger, and the heat exchanger physical dimensions. The flow path areas affect how air is compressed through the bypass duct, which in turn affects the flow temperature. Higher fuel temperatures increase the amount of heat dissipated through the heat exchanger. The number of cross-flow channels, the fin thickness, height, and width, on both the hot and cold sides of the heat exchanger affects the heat dissipation ability. However, for the studies presented in this paper, we hold the physical heat exchanger design parameters fixed. Given that the physical design parameters are fixed, heat exchanger performance depends on the fuel and air flow rates, which are dictated by the optimizer and the aircraft speed, respectively.

2.5. Multidisciplinary Model Setup

We combine the individual disciplinary models into a fully coupled multidisciplinary model as shown by Figure 6. The coupling between the flight dynamics, aerodynamics, and propulsion analysis blocks is resolved through a Newton solver.

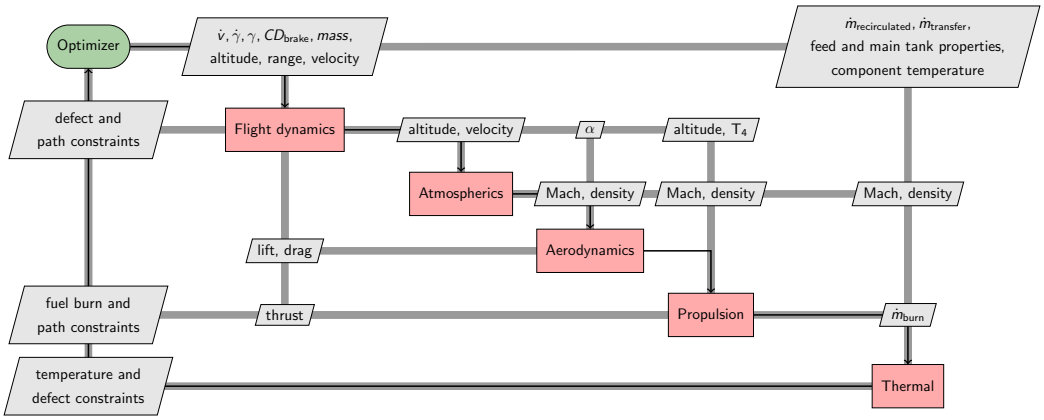

Figure 6. XDSM diagram [60] of the fully-coupled problem, including the optimizer, design variables, and constraints.

The flight dynamics, tank temperature and masses, and electrical component temperatures are integrated using the Legendre–Gauss–Radau implicit collocation scheme at the optimizer level. Collocation schemes ensure that the optimized result produces a physically accurate time history through constraints on values called *defects*. The difference between the slope of the interpolative collocation function and the physics-based rate for the state of interest is called a *defect* and must be

constrained to equal 0 at the optimal design point. These defect constraints are added to the top-level optimization problem.

Implicit collocation schemes are well-suited for gradient-based optimization for two main reasons [27]. First, they pose optimal control problems in a way that the number of calculations performed each iteration is constant. This is important so the optimization problem size does not change during the course of solving the optimization problem. Secondly, these collocation schemes produce sparse Jacobian structures, which means that large-scale problems can be solved efficiently by reducing computational cost. OpenMDAO is designed to take advantage of this sparsity, especially when computing the total derivatives of the problem.

3. Optimization Methodology and Formulation

3.1. Optimization Framework: OpenMDAO

Throughout this work, we use OpenMDAO (https://github.com/openmdao/openmdao) [61] as the underlying optimization framework. OpenMDAO was developed at NASA Glenn and uses the MAUD theory to allow for modular construction and execution of complicated models [47]. OpenMDAO has been used to optimize a huge variety of problems, including thermodynamic engine cycles [57,58,62,63] and MDO of aircraft considering mission performance [28,39,40,64].

Many features of OpenMDAO directly enabled the research presented in this paper. Model construction was greatly simplified by the ability to connect analysis blocks easily from different tools. Tools for model layout visualization and debugging that come packaged with OpenMDAO decreased the time to set up and verify the problem. Solver convergence information and model debugging tools helped us determine what to fix when the model did not converge successfully. Additionally, multiple open-source tools have been written using OpenMDAO and were directly used in this work, including Dymos (https://github.com/openmdao/dymos) [27] for mission optimization and pyCycle (https://github.com/openmdao/pycycle) [57] for engine design. These tools and features make OpenMDAO a useful and necessary tool for setting up, analyzing, and optimizing multidisciplinary systems efficiently within this paper.

Within this work, we use pyOptSparse [65] and SNOPT [66]. pyOptSparse (https://github.com/mdolab/pyoptsparse) is an open-source Python framework that provides a common interface for many gradient-based and gradient-free optimization methods. SNOPT is a sequential quadratic programming approach that efficiently solves large sparse nonlinear constrained optimization problems [66]. OpenMDAO has native support for pyOptSparse and any of its wrapped optimization methods.

3.2. Mission Integration Tool: Dymos

In this paper, we use Dymos (https://github.com/openmdao/dymos) to solve the path-dependent MDO problems. Dymos [27] is an open-source tool built upon OpenMDAO. It provides an interface for integration of ODEs with MDO in mind.

Dymos' implementation is based in part on NASA's OTIS optimal control software [67]. Dymos contains both high-order pseudospectral collocation methods and Runge–Kutta schemes and provides convenient user-facing methods to solve optimal control and design problems. Dymos has been used to optimize aircraft trajectories in parallel [68], aircraft trajectories with propulsion in the loop [25], and next generation aircraft concepts [24,28,69].

Dymos breaks a trajectory into one or more *phases*, and then each of those phases into *segments*. These segments are modeled as a polynomial and values of the states and controls are considered at *nodes* across these segments. Boundary or path constraints can be used on any output from the model, regardless if it is a state or not. In this work, we use multiple phases for the ascent, cruise, and descent portions of the mission and link the time, states, and controls to ensure continuity.

4. Optimization Problem Results

4.1. Thermally-Constrained Mission Optimization

With a better understanding of the fully coupled model and its design space, we introduce the optimization problem formulation in this subsection. Table 3 has the complete optimization problem formulation for a reconnaissance mission. Here, we are minimizing the fuel burn for a supersonic mission where the cruise Mach number and altitude are prescribed and the ascent and descent profiles are optimized. Two optimization cases are presented: one without and one with thermal constraints and thermal design variables.

Table 3. Optimization problem formulations for the fully-coupled supersonic reconnaissance mission.

Category	Name	Quantity		Lower	Upper	Units
		No Thermal Constraints	Thermal Constraints			
Objective	fuel burn	1	1	–	–	kg
Variables	$\dot{\gamma}$	12	12	−0.1	0.1	radians/s
	$\dot{v}$	12	12	−5	5	m/s^2
	CD_{brake}	6	6	0	0.05	
	$\dot{m}_{\text{recirculated}}$	0	18	0	10	kg/s
	$\dot{m}_{\text{transfer}}$	0	18	0	10	kg/s
	mass	83	83	15,000	30,000	kg
	altitude	83	83	0	16	km
	range	83	83	0	–	km
	velocity	83	83	0	1000	m/s
	γ	82	82	−0.5	0.5	radians
	feed mass	83	83	10	–	kg
	main mass	83	83	10	–	kg
	feed T	83	83	100	1000	K
	main T	83	83	100	1000	K
	component T	83	83	100	1000	K
	m_{pumped}	83	83	–	–	kg
	Total	**944**	**980**			
Constraints	final altitude	1	1	100	100	m
	final Mach	1	1	0.	0.5	
	Mach cruise path constraints	36	36	1.4	1.4	
	altitude cruise path constraints	36	36	13	13	km
	α path constraints	84	84	−15	15	degrees
	T_4 path constraints	84	84	2000	3200	degrees R
	CD_{brake}	24	24	0	–	
	$\dot{m}_{\text{recirculated}}$ path constraints	0	84	0.01	–	kg/s
	feed mass path constraints	0	84	500	–	kg
	$\dot{m}_{\text{transfer}}$ path constraints	0	84	0	–	kg/s
	T_{out} path constraints	0	84	–	100	degrees C
	Component T path constraints	0	84	–	80	degrees C
	main T path constraints	0	84	300	300	K
	range defects	70	70	0	0	km
	altitude defects	70	70	0	0	km
	velocity defects	70	70	0	0	m/s
	γ defects	70	70	0	0	radians
	mass defects	70	70	0	0	kg
	feed mass defects	70	70	0	0	kg
	feed T defects	70	70	0	0	K
	main T defects	70	70	0	0	K
	component T defects	70	70	0	0	K
	m pumped defects	70	70	0	0	kg
	main mass defects	70	70	0	0	kg
	phase continuity constraints	121	121	0	0	
	linkage constraints	24	24	0	0	
	Total	**1181**	**1685**			

The first case, labeled as "No thermal constraints" in the table, finds the optimal mission without considering the performance of the thermal system, though the thermal states are tracked. The second case, labeled as "Thermal constraints" in the table, includes thermal constraints and thermal design variables. Here, the temperature of the cooled avionics component and the fuel temperature are limited to prevent electronics degradation and fuel overheat, respectively. We would expect the optimizer to increase the fuel flow through the thermal system to better cool the component, or take a different flight path to access air at a lower temperature for the ducted heat exchanger in this problem.

The thermal load coming from the avionics component is set at 20 kW for the ascent and descent phases, and 30 kW for the cruise phase to simulate increased thermal load due to the use of a reconnaissance sensor. The ascent, cruise, and descent time durations are set to 200, 1000, and 200 s, respectively. For the case without thermal constraints, the recirculatory flow rate is $\dot{m}_{\text{recirculated}} = 1.0$ kg/s and the main-to-feed tank transfer rate is $\dot{m}_{\text{transfer}} = 1.0$ kg/s and both are fixed across the mission. The initial feed tank fuel mass is 1000 kg and the initial temperatures for the main tank, feed tank, and component are all 300 K in both cases.

As highlighted in Table 3, these optimization problems are relatively large, as the thermal case has 980 design variables and 1602 functions of interest. These optimization studies are partially enabled by OpenMDAO's sparse coloring algorithms [70]. For the thermal case, coloring reduces the number of independent sensitivity analysis calls from 980 to 258, resulting in a 73.7% improvement in computational cost. This helps to decrease the time between optimization cases and design iterations to increase the rate that the large design space can be explored by experts.

Figure 7 shows the optimal results of these two cases. Without thermal constraints, the full mission fuel burn is 2323.7 kg, whereas the aircraft burns 2880.9 kg of fuel for the thermally-constrained mission. Examining the case without thermal constraints first, the optimal altitude profile has a straightforward ascent profile where the aircraft accelerates for a short time before climbing the cruise altitude and then accelerating further to the prescribed cruise Mach number. The component temperature increases and reaches steady-state in the ascent phase before increasing when the sensor thermal load is introduced for the cruise phase. The thermal constraint, shown by a gray line on the component temperature axes in Figure 7, is violated for the entire cruise phase and is only satisfied shortly after the descent phase begins. Because the descent time duration is fixed at 200 s, the aircraft briefly increases altitude while losing speed before continuing its descent.

For the thermally-constrained case, the optimal ascent profile is markedly different than for the unconstrained case. The aircraft focuses on gaining speed instead of altitude to force more air through the ducted heat exchanger, which increases the amount of thermal energy that can be dissipated. This requires the engine to be at full throttle through the ascent at a lower altitude, which is responsible for the increase in fuel burn compared to the thermally-unconstrained case. The increased fuel flow also increases the amount of thermal energy dissipated through the heat exchanger. After reaching Mach 1.5, the aircraft climbs to the cruise altitude and in the process slows to the prescribed cruise Mach number of 1.4. This allows the component and feed tank temperatures to be lower than in the unconstrained case. Although tailoring the flight path helps the thermal system, there are no feasible solutions to this thermally-constrained problem unless the optimizer can also control the recirculated fuel flow rate. The $C1$-discontinuous component temperature trends are caused by prescribed changes in the thermal load corresponding to increased electronic usage during the cruise phase.

During the ascent phase, the optimizer also increases $\dot{m}_{\text{recirculated}}$ to increase the fuel flow rate through the component and ducted heat exchangers to dissipate more thermal energy. This, coupled with the lower feed tank temperature due to the ascent profile, helps keep the component temperature below its upper limit. In the problem presented here, there are multiple feasible answers because the thermal constraints can be met through multiple fuel flow histories. Although we are not capturing the added energy cost of pumping fuel as coolant in the thermal system, introducing that coupling would affect the optimal $\dot{m}_{\text{recirculated}}$ profile and reduce the number of feasible solutions. This optimization problem is dependent on having a good initial starting condition due to the collocation scheme.

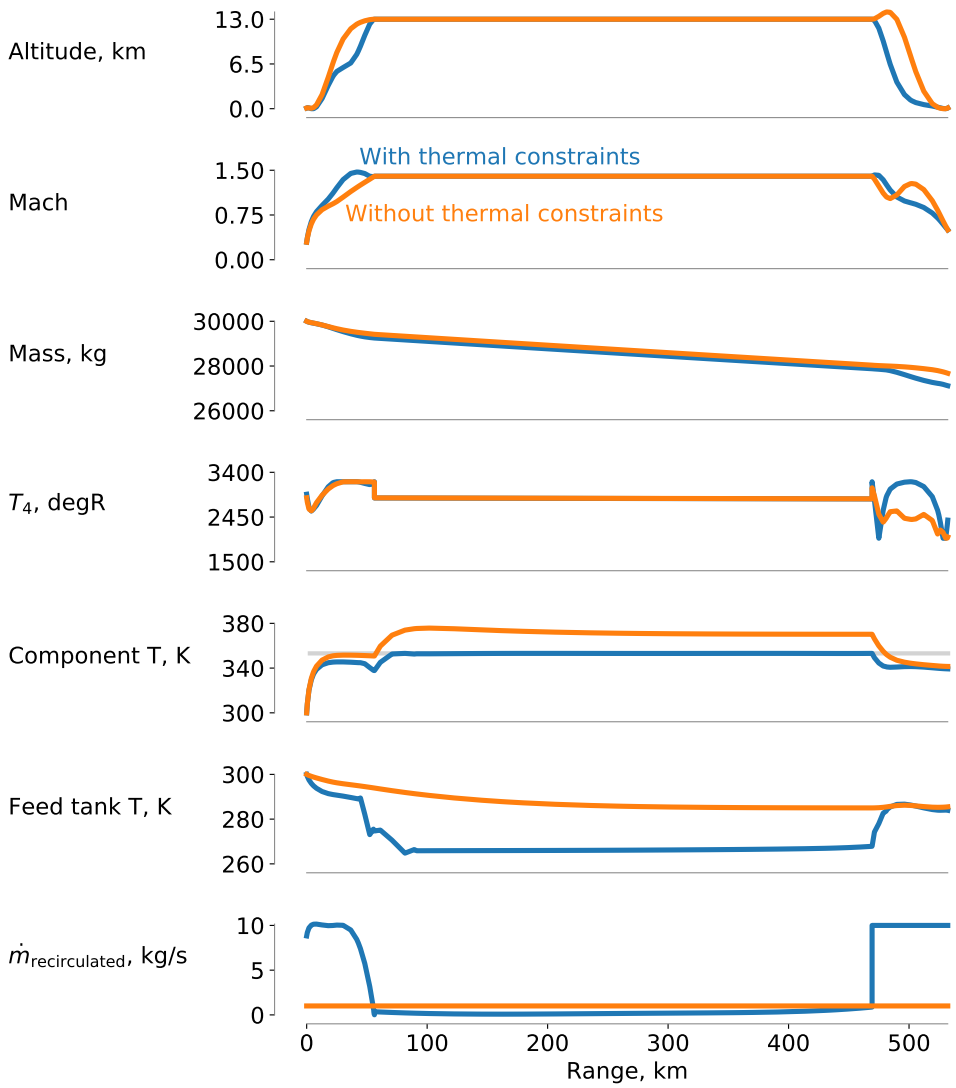

Figure 7. Without thermal constraints on the system, the optimal mission takes a more direct ascent profile. In the thermally-constrained case, the optimizer chooses to more quickly increase speed to force more air through the ducted heat exchanger to dissipate more heat in the ascent phase. The thermal constraint for the avionic component temperature is shown in light gray.

4.2. Cruise-Mission Endurance Optimization

Lastly, we examine the optimal flight profiles when the optimizer has more freedom to tailor the mission. Here we track the thermal system states but do not constrain the optimization problem based on these states. Instead, we focus on the optimal flight path given the additional freedom in speed and altitude profiles as a measure of endurance mission performance.

Without prescribing the Mach number and altitude profiles for the cruise phase, we would expect a lower fuel burn. Figure 8 shows the thermally-unconstrained case from before and the optimal result from a more flexible problem formulation with the cruise requirements removed. The x-axis is time, not range, so the total distance traveled in the two missions is not necessarily equal. The ascent, cruise, and descent phases again have fixed durations of 200, 1000, and 200 s, respectively.

With the additional flexibility, the optimizer rounds out the altitude profile and takes a more conservative flight path. Without the prescribed cruise Mach number, the more flexible mission cruises in the transonic regime, which is more fuel efficient. This more efficient profile results in a fuel burn of 1617.6 kg, compared to the 2323.7 kg for the constrained cruise case. By formulating the problem such that the aircraft flies for the same duration as the previous problem, we see how the optimizer changes

the flight profile to maximize endurance by lowering fuel burn. We are not constraining the thermal system here, so the optimized flight profiles do not depend on thermal dissipation performance. Instead, we focus on the degrees of freedom available in this optimization problem and the additional performance afforded in relaxing constraints.

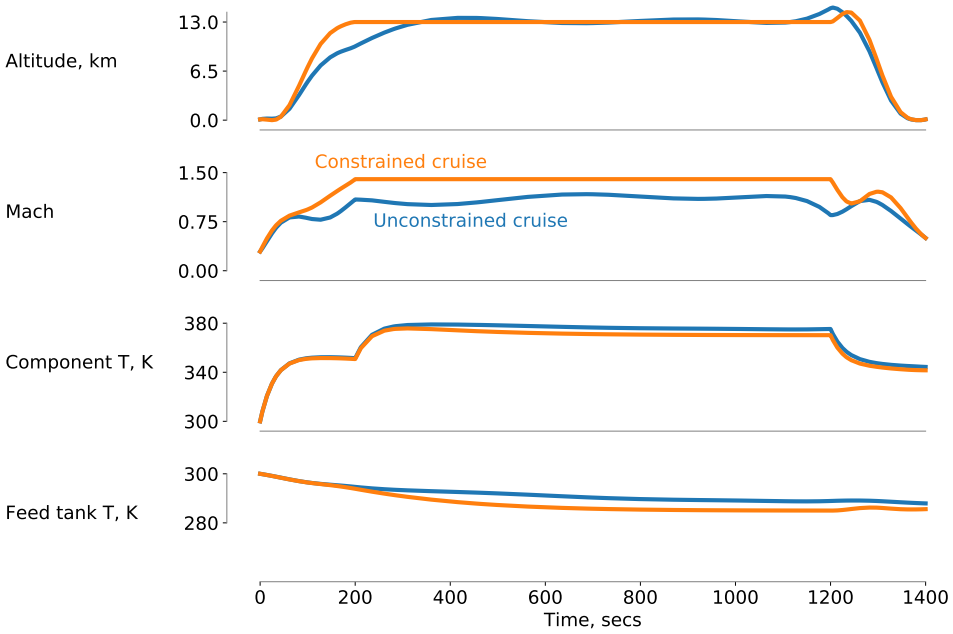

Figure 8. Without the Mach and altitude constraints on the cruise phase, the optimizer takes a more conservative ascent profile and cruise at a lower Mach number. The x-axis here is time, so the two aircraft do not fly the same total distance due to their different flight speeds.

5. Conclusions

Large-scale path-dependent optimization problems are challenging to solve due to their high dimensional design space. In this paper, we present methods to reduce the computational cost of solving these multidisciplinary problems. We do this by constructing a general methodology that can track path-dependent states from multiple disciplines through a flight trajectory.

We demonstrate this methodology's capability by constructing a coupled aero-thermal-propulsive-mission multidisciplinary model to optimize a supersonic aircraft considering its path-dependent performance with thermal constraints. The optimization problems include on the order of 1000 design variables and 1000 constraints. We present results for the optimal flight trajectory considering thermal constraints and discuss the non-intuitive optimal design trends. We also present optimal flight trajectories with fewer path constraints to show the flexibility of the methodology. This paper is useful for researchers considering any combination of path-dependent optimization and large-scale MDO problems.

The path-dependent optimization process detailed in this paper can be used to assess and design other aircraft and missions. Other missions of interest might arise in urban air mobility, supersonic combat, radar area coverage, or firefighting missions. Achieving optimal performance for each of these missions requires designers to consider specific path-dependent states during the design optimization process. These new aircraft configurations might have non-intuitive coupling between subsystems that can be efficiently evaluated using the methods presented in this paper.

Author Contributions: Writing—review and editing, J.P.J., J.S.G., B.J.B., C.A.M., J.R.R.A.M.; conceptualization J.P.J., J.S.G., C.A.M., J.R.R.A.M.; methodology, software J.P.J., C.A.M., B.J.B., J.S.G.; validation, investigation, data curation J.P.J., J.S.G.; formal analysis, writing—original draft preparation, visualization J.P.J.; resources, supervision, project administration, funding acquisition C.A.M., J.R.R.A.M. All authors have read and agreed to the published version of the manuscript.

Funding: The first and second authors are grateful for support from the National Science Foundation Graduate Research Fellowship under Grant No. DGE-1256260. The first author is also grateful for support from the University of Michigan Rackham Pre-Doctoral Fellowship. The work presented in this paper is partially supported by NASA's Transformative Tools and Technologies Project. This work was also supported by the U.S. Air Force Research Laboratory (AFRL) under the Michigan–AFRL Collaborative Center in Aerospace Vehicle Design.

Acknowledgments: The authors thank Jon Seidel at NASA Glenn Research Center for his assistance in constructing and understanding the engine model.

Conflicts of Interest: The authors declare no conflict of interest.

Abbreviations

The following abbreviations are used in this manuscript:

MDO	multidisciplinary design optimization
FTMS	fuel thermal management system
CFD	computational fluid dynamics
AFRL	Air Force Research Laboratory
TMS	thermal management system
RANS	Reynolds-averaged Navier–Stokes
ODE	ordinary differential equation
ESAV	Efficient Supersonic Air Vehicle
SMT	Surrogate Modeling Toolbox
NPSS	Numerical Propulsion System Simulation

References

1. Kaiser, F. *The Climb of Jet-Propelled Aircraft, Part I. Speed Along the Path of Optimum Climb*; RTP/TIB Translation No. Tech. Rep. GDC/15/14ST; Ministry of Supply (Gt. Brit.): London, UK; 1944.
2. Faulders, C. *Low-Thrust Rocket Steering Program for Minimum Time Transfer between Planetary Orbits*; Technical Report; SAE Technical Paper: Warrendale, PA, USA, 1958.
3. Bryson, A.E., Jr.; Ross, S.E. Optimum rocket trajectories with aerodynamic drag. *J. Jet Propuls.* **1958**, *28*, 465–469. [CrossRef]
4. Kelley, H.J. Gradient theory of optimal flight paths. *ARS J.* **1960**, *30*, 947–954. [CrossRef]
5. Kelley, H.J. An investigation of optimal zoom climb techniques. *J. Aerosp. Sci.* **1959**, *26*, 794–802. [CrossRef]
6. Bryson, A.E.; Denham, W.F. A steepest-ascent method for solving optimum programming problems. *J. Appl. Mech.* **1962**, *29*, 247–257. [CrossRef]
7. Bryson, A.E. Optimal control-1950 to 1985. *IEEE Control Syst. Mag.* **1996**, *16*, 26–33. [CrossRef]
8. Hale, A.L.; Dahl, W.; Lisowski, J. Optimal simultaneous structural and control design of maneuvering flexible spacecraft. *J. Guid. Control Dyn.* **1985**, *8*, 86–93. [CrossRef]
9. Miller, D.F.; Shim, J. Gradient-based combined structural and control optimization. *J. Guid. Control Dyn.* **1987**, *10*, 291–298. [CrossRef]
10. Belvin, W.K.; Park, K. Structural tailoring and feedback control synthesis-An interdisciplinary approach. *J. Guid. Control Dyn.* **1990**, *13*, 424–429. [CrossRef]
11. Onoda, J.; Haftka, R.T. An approach to structure/control simultaneous optimization for large flexible spacecraft. *AIAA J.* **1987**, *25*, 1133–1138. [CrossRef]
12. Clive, P.D.; Johnson, J.A.; Moss, M.J.; Zeh, J.M.; Birkmire, B.M.; Hodson, D.D. Advanced Framework for Simulation, Integration and Modeling (AFSIM)(Case Number: 88ABW-2015-2258). In Proceedings of the International Conference on Scientific Computing (CSC). The Steering Committee of The World Congress in Computer Science, Computer, Las Vegas, NV, USA, 27–30 July 2015; p. 73.
13. Reuter, R.A.; Iden, S.; Snyder, R.D.; Allison, D.L. An overview of the optimized integrated multidisciplinary systems program. In Proceedings of the 57th AIAA/ASCE/AHS/ASC Structures, Structural Dynamics, and Materials Conference, San Diego, CA, USA, 4–8 January 2016; p. 0674.
14. Alyanak, E.J.; Allison, D.L. Multi-Parameter Performance Evaluation, the Next Step in Conceptual Design Concept Assessment. In Proceedings of the 56th AIAA/ASCE/AHS/ASC Structures, Structural Dynamics, and Materials Conference, Kissimmee, FL, USA, 5–9 January 2015; p. 0648.

15. Allison, D.L.; Kolonay, R.M. Expanded MDO for Effectiveness Based Design Technologies: EXPEDITE Program Introduction. In Proceedings of the 2018 Multidisciplinary Analysis and Optimization Conference, Atlanta, GA, USA, 25–29 June 2018; p. 3419.
16. Davies, C.C. Lockheed Martin Overview of the AFRL EXPEDITE Program. In Proceedings of the AIAA Scitech 2019 Forum, San Diego, CA, USA, 7–11 January 2019; p. 0173.
17. Clark, D.L., Jr.; Allison, D.L.; Bae, H.; Forster, E.E. Effectiveness-Based Design of an Aircraft Considering Mission Uncertainties. *J. Aircr.* **2019**, *56*, 1–12. [CrossRef]
18. Bodie, M.; Russell, G.; McCarthy, K.; Lucas, E.; Zumberge, J.; Wolff, M. Thermal analysis of an integrated aircraft model. In Proceedings of the 48th AIAA Aerospace Sciences Meeting Including the New Horizons Forum and Aerospace Exposition, Orlando, FL, USA, 4–7 January 2010; p. 288.
19. Alyanak, E.J.; Allison, D.L. Fuel Thermal Management System Consideration in Conceptual Design Sizing. In Proceedings of the 57th AIAA/ASCE/AHS/ASC Structures, Structural Dynamics, and Materials Conference, San Diego, CA, USA, 4–8 January 2016; p. 0670.
20. Klatt, N.D. *On-Board Thermal Management of Waste Heat from a High-Energy Device*; Technical Report; Air Force Institute of Technology at Wright-Patterson Air Force Base: Dayton, OH, USA, 2008.
21. DeSimio, M.P.; Hencey, B.M.; Parry, A.C. Online prognostics for fuel thermal management system. In Proceedings of the ASME 2015 Dynamic Systems and Control Conference, Columbus, OH, USA, 28–30 October 2015; American Society of Mechanical Engineers: New York, NY, USA, 2015; p. V001T08A003.
22. Gvozdich, G.; Weise, P.; von Spakovsky, M. INVENT: Study of the Issues Involved in Integrating a Directed Energy Weapons Subsystem into a High Performance Aircraft System. In Proceedings of the 50th AIAA Aerospace Sciences Meeting including the New Horizons Forum and Aerospace Exposition, Nashville, TN, USA, 9–12 January 2012; p. 490.
23. Wolff, M. INVENT Tip to Tail Energy/Engine/Power/Thermal Modeling, Simulation, & Analysis (MS&A). In Proceedings of the 5th Annual Research Consortium for Multidisciplinary System Design Workshop, Boston, MA, USA, 15–16 July 2010.
24. Falck, R.D.; Chin, J.; Schnulo, S.L.; Burt, J.M.; Gray, J.S. Trajectory Optimization of Electric Aircraft Subject to Subsystem Thermal Constraints. In Proceedings of the 18th AIAA/ISSMO Multidisciplinary Analysis and Optimization Conference, Denver, CO, USA, 5–9 June 2017. [CrossRef]
25. Hendricks, E.S.; Falck, R.D.; Gray, J.S. Simultaneous Propulsion System and Trajectory Optimization. In Proceedings of the 18th AIAA/ISSMO Multidisciplinary Analysis and Optimization Conference, Denver, CO, USA, 5–9 June 2017; p. AIAA-2017-4435. [CrossRef]
26. Schnulo, S.L.; Jeff Chin, R.D.F.; Gray, J.S.; Papathakis, K.V.; Clarke, S.C.; Reid, N.; Borer, N.K. Development of a Multi-Segment Mission Planning Tool for SCEPTOR X-57. In Proceedings of the 2018 Multidisciplinary Analysis and Optimization Conference, Atlanta, GA, USA, 25–29 June 2018. [CrossRef]
27. Falck, R.D.; Gray, J.S. Optimal control within the context of multidisciplinary design, analysis, and optimization. In Proceedings of the AIAA Scitech 2019 Forum, San Diego, CA, USA, 7–11 January 2019. [CrossRef]
28. Hendricks, E.S.; Falck, R.D.; Gray, J.S.; Aretskin-Hariton, E.D.; Ingraham, D.J.; CHapman, J.W.; Schnulo, S.L.; Chin, J.C.; Jasa, J.P.; Bergeson, J.D. Multidisciplinary Optimization of a Turboelectric Tiltwing Urban Air Mobility Aircraft. In Proceedings of the AIAA/ISSMO Multidisciplinary Analysis and Optimization Conference, Dallas, TX, USA, 17–21 June 2019.
29. Liem, R.P.; Mader, C.A.; Lee, E.; Martins, J.R.R.A. Aerostructural design optimization of a 100-passenger regional jet with surrogate-based mission analysis. In Proceedings of the 2013 Aviation Technology, Integration, and Operations Conference, Los Angeles, CA, USA, 12–14 August 2013. [CrossRef]
30. Kao, J.Y.; Hwang, J.T.; Martins, J.R.R.A.; Gray, J.S.; Moore, K.T. A Modular Adjoint Approach to Aircraft Mission Analysis and Optimization. In Proceedings of the AIAA Science and Technology Forum and Exposition (SciTech), Kissimmee, FL, USA, 5–9 January 2015. p. AIAA 2015-0136.
31. Kao, J.Y.; Hwang, J.T.; Martins, J.R.R.A. A Modular Approach for Mission Analysis and Optimization. In Proceedings of the 56th AIAA/ASME/ASCE/AHS/ASC Structures, Structural Dynamics, and Materials Conference, Kissimmee, FL, USA, 5–9 January 2015.
32. Liem, R.P. Multimission Fuel-Burn Minimization in Aircraft Design: A Surrogate-Modeling Approach. Ph.D. Thesis, University of Toronto, Toronto, ON, Canada, 2015.

33. Hwang, J.T.; Jasa, J.; Martins, J.R.R.A. High-fidelity design-allocation optimization of a commercial aircraft maximizing airline profit. *J. Aircr.* **2019**, *56*, 1165–1178. [CrossRef]
34. Liem, R.P.; Mader, C.A.; Martins, J.R.R.A. Surrogate Models and Mixtures of Experts in Aerodynamic Performance Prediction for Aircraft Mission Analysis. *Aerosp. Sci. Technol.* **2015**, *43*, 126–151. [CrossRef]
35. Liem, R.P.; Kenway, G.K.W.; Martins, J.R.R.A. Multimission Aircraft Fuel Burn Minimization via Multipoint Aerostructural Optimization. *AIAA J.* **2015**, *53*, 104–122. [CrossRef]
36. Brelje, B.J.; Martins, J.R.R.A. Development of a Conceptual Design Model for Aircraft Electric Propulsion with Efficient Gradients. In Proceedings of the AIAA/IEEE Electric Aircraft Technologies Symposium, Cincinnati, OH, USA, 9–11 July 2018. [CrossRef]
37. Brelje, B.J.; Jasa, J.P.; Martins, J.R.R.A.; Gray, J.S. Development of a Conceptual-Level Thermal Management System Design Capability in OpenConcept. In *NATO Research Symposium on Hybrid/Electric Aero-Propulsion Systems for Military Applications*; AVT-RSY-323; NATO: Brussels, Belgium, 2019. [CrossRef]
38. Chauhan, S.S.; Martins, J.R.R.A. Tilt-wing eVTOL takeoff trajectory optimization. *J. Aircr.* **2020**, *57*, 93–112. [CrossRef]
39. Jasa, J.P.; Hwang, J.T.; Martins, J.R.R.A. Design and Trajectory Optimization of a Morphing Wing Aircraft. In Proceedings of the 2018 AIAA/ASCE/AHS/ASC Structures, Structural Dynamics, and Materials Conference, Kissimmee, FL, USA, 8–12 January 2018. [CrossRef]
40. Jasa, J.P.; Mader, C.A.; Martins, J.R.R.A. Trajectory Optimization of a Supersonic Air Vehicle with Thermal Fuel Management System. In Proceedings of the AIAA/ISSMO Multidisciplinary Analysis and Optimization Conference, Atlanta, GA, USA, 25–29 June 2018. [CrossRef]
41. Marta, A.C.; Mader, C.A.; Martins, J.R.R.A.; van der Weide, E.; Alonso, J.J. A methodology for the development of discrete adjoint solvers using automatic differentiation tools. *Int. J. Comput. Fluid Dyn.* **2007**, *21*, 307–327. [CrossRef]
42. Mader, C.A.; Martins, J.R.R.A.; Alonso, J.J.; van der Weide, E. ADjoint: An Approach for the Rapid Development of Discrete Adjoint Solvers. *AIAA J.* **2008**, *46*, 863–873. [CrossRef]
43. Kenway, G.K.W.; Mader, C.A.; He, P.; Martins, J.R.R.A. Effective Adjoint Approaches for Computational Fluid Dynamics. *Prog. Aerosp. Sci.* **2019**, *110*, 100542. [CrossRef]
44. Kenway, G.K.W.; Martins, J.R.R.A. Multipoint High-Fidelity Aerostructural Optimization of a Transport Aircraft Configuration. *J. Aircr.* **2014**, *51*, 144–160. [CrossRef]
45. Martins, J.R.R.A.; Hwang, J.T. Review and Unification of Methods for Computing Derivatives of Multidisciplinary Computational Models. *AIAA J.* **2013**, *51*, 2582–2599. [CrossRef]
46. Martins, J.R.R.A.; Lambe, A.B. Multidisciplinary Design Optimization: A Survey of Architectures. *AIAA J.* **2013**, *51*, 2049–2075. [CrossRef]
47. Hwang, J.T.; Martins, J.R.R.A. A computational architecture for coupling heterogeneous numerical models and computing coupled derivatives. *ACM Trans. Math. Softw.* **2018**, *44*, 37. [CrossRef]
48. Allison, D.; Morris, C.; Schetz, J.; Kapania, R.; Sultan, C.; Deaton, J.; Grandhi, R. A multidisciplinary design optimization framework for design studies of an efficient supersonic air vehicle. In Proceedings of the 12th AIAA Aviation Technology, Integration, and Operations (ATIO) Conference and 14th AIAA/ISSMO Multidisciplinary Analysis and Optimization Conference, Indianapolis, IN, USA, 17–19 September 2012; p. 5492. [CrossRef]
49. Burton, S.; Alyanak, E.; Kolonay, R. Efficient supersonic air vehicle analysis and optimization implementation using SORCER. In Proceedings of the 12th AIAA Aviation Technology, Integration, and Operations (ATIO) Conference and 14th AIAA/ISSMO Multidisciplinary Analysis and Optimization Conference, Indianapolis, IN, USA, 17–19 September 2012; p. 5520. [CrossRef]
50. Alyanak, E.; Kolonay, R. Efficient supersonic air vehicle structural modeling for conceptual design. In Proceedings of the 12th AIAA Aviation Technology, Integration, and Operations (ATIO) Conference and 14th AIAA/ISSMO Multidisciplinary Analysis and Optimization Conference, Indianapolis, IN, USA, 17–19 September 2012; p. 5519. [CrossRef]
51. Davies, C.; Stelmack, M.; Zink, P.S.; De La Garza, A.; Flick, P. High fidelity MDO process development and application to fighter strike conceptual design. In Proceedings of the 12th AIAA Aviation Technology, Integration, and Operations (ATIO) Conference and 14th AIAA/ISSMO Multidisciplinary Analysis and Optimization Conference, Indianapolis, IN, USA, 17–19 September 2012; p. 5490. [CrossRef]

52. Mader, C.A.; Kenway, G.K.W.; Yildirim, A.; Martins, J.R.R.A. ADflow—An open-source computational fluid dynamics solver for aerodynamic and multidisciplinary optimization. *J. Aerosp. Inf. Syst.* **2020**. [CrossRef]
53. Secco, N.R.; Jasa, J.P.; Kenway, G.K.W.; Martins, J.R.R.A. Component-based Geometry Manipulation for Aerodynamic Shape Optimization with Overset Meshes. *AIAA J.* **2018**, *56*, 3667–3679. [CrossRef]
54. Yildirim, A.; Kenway, G.K.W.; Mader, C.A.; Martins, J.R.R.A. A Jacobian-free approximate Newton–Krylov startup strategy for RANS simulations. *J. Comput. Phys.* **2019**, *397*, 108741. [CrossRef]
55. Bouhlel, M.A.; Hwang, J.T.; Bartoli, N.; Lafage, R.; Morlier, J.; Martins, J.R.R.A. A Python surrogate modeling framework with derivatives. *Adv. Eng. Softw.* **2019**, *135*, 102662. [CrossRef]
56. Hwang, J.T.; Martins, J.R.R.A. A fast-prediction surrogate model for large datasets. *Aerosp. Sci. Technol.* **2018**, *75*, 74–87. [CrossRef]
57. Hendricks, E.S.; Gray, J.S. pyCycle: A Tool for Efficient Optimization of Gas Turbine Engine Cycles. *Aerospace* **2019**, *6*, 87. [CrossRef]
58. Gray, J.S.; Chin, J.; Hearn, T.; Hendricks, E.; Lavelle, T.; Martins, J.R.R.A. Chemical Equilibrium Analysis with Adjoint Derivatives for Propulsion Cycle Analysis. *J. Propuls. Power* **2017**, *33*, 1041–1052. [CrossRef]
59. Bruno, T.J. *Thermodynamic, Transport and Chemical Properties of Reference JP-8*; Technical Report; National Institute of Standards and Technology: Boulder, CO, USA, 2006.
60. Lambe, A.B.; Martins, J.R.R.A. Extensions to the Design Structure Matrix for the Description of Multidisciplinary Design, Analysis, and Optimization Processes. *Struct. Multidiscip. Optim.* **2012**, *46*, 273–284. [CrossRef]
61. Gray, J.S.; Hwang, J.T.; Martins, J.R.R.A.; Moore, K.T.; Naylor, B.A. OpenMDAO: An open-source framework for multidisciplinary design, analysis, and optimization. *Struct. Multidiscip. Optim.* **2019**, *59*, 1075–1104. [CrossRef]
62. Jasa, J.P.; Brelje, B.J.; Mader, C.A.; Martins, J.R.R.A. Coupled Design of a Supersonic Engine and Thermal System. In Proceedings of the World Congress of Structural and Multidisciplinary Optimization, Beijing, China, 20–24 May 2019.
63. Hearn, T.A.; Hendricks, E.; Chin, J.; Gray, J.S. Optimization of Turbine Engine Cycle Analysis with Analytic Derivatives. In Proceedings of the 17th AIAA/ISSMO Multidisciplinary Analysis and Optimization Conference, Washington, DC, USA, 13–17 June 2016. [CrossRef]
64. Jasa, J.P. Multidisciplinary Design Optimization of an Aircraft Considering Path-Dependent Performance. Ph.D. Thesis, University of Michigan, Ann Arbor, MI, USA, 2019.
65. Perez, R.E.; Jansen, P.W.; Martins, J.R.R.A. pyOpt: A Python-Based Object-Oriented Framework for Nonlinear Constrained Optimization. *Struct. Multidiscip. Optim.* **2012**, *45*, 101–118. [CrossRef]
66. Gill, P.E.; Murray, W.; Saunders, M.A. SNOPT: An SQP algorithm for large-scale constrained optimization. *SIAM J. Optim.* **2002**, *12*, 979–1006. [CrossRef]
67. Hargraves, C.R.; Paris, S.W. Direct trajectory optimization using nonlinear programming and collocation. *J. Guid. Control Dyn.* **1987**, *10*, 338–342. [CrossRef]
68. Falck, R.D.; Gray, J.S.; Naylor, B. Parallel aircraft trajectory optimization with analytic derivatives. In Proceedings of the 17th AIAA/ISSMO Multidisciplinary Analysis and Optimization Conference, Washington, DC, USA, 13–17 June 2016; p. 3207.
69. Falck, R.D.; Ingraham, D.; Aretskin-Hariton, E. Multidisciplinary Optimization of Urban-Air-Mobility Class Aircraft Trajectories with Acoustic Constraints. In Proceedings of the 2018 AIAA/IEEE Electric Aircraft Technologies Symposium, Cincinnati, OH, USA, 9–11 July 2018. [CrossRef]
70. Gray, J.S.; Hearn, T.A.; Naylor, B.A. Using Graph Coloring To Compute Total Derivatives More Efficiently in OpenMDAO. In Proceedings of the AIAA Aviation 2019 Forum, Dallas, TX, USA, 17–21 June 2019; p. 3108. [CrossRef]